Shock Waves (2005) 14(4): 307–311
DOI 10.1007/s00193-005-0255-8

TECHNICAL NOTE

T. I. Tseng · R. J. Yang

Simulation of the Mach reflection in supersonic flows by the CE/SE method

Received: 10 December 2004 / Revised: 10 December 2004 / Accepted: 28 March 2005 / Published online: 29 September 2005

Abstract This study employs the Space-Time Conservation Element and Solution Element (CE/SE) method to determine the influence of downstream flow conditions on Mach stem height. The results indicate that the Mach stem height depends on the incident shock wave angle and the distance between the trailing edge and the symmetry plane. Furthermore, it is shown that the downstream length ratio and the trailing edge angle do not affect the Mach stem height nor the Mach reflection (MR) configuration, and the Space-Time Conservation Element and Solution Element method is able to simulate the MR as well as many other numerical schemes.

Keywords Supersonic flow · Mach reflection · Mach stem height · CE/SE method

PACS 47.40.Nm

1 Introduction

Two shock wave reflection configurations are possible in steady supersonic flows, namely Regular Reflection (RR) and Mach Reflection (MR). In general, the MR configuration can be described by applying three-shock theory in the vicinity of the triple point. If any point along the incident shock wave is selected and three lines are drawn parallel to the reflected shock wave, Mach stem and slipstream, respectively, then a new triple point can be obtained. The two triple points completely satisfy three-shock theory. Hence, it is clear that multiple MR configurations exist for any given set of flow conditions. However, this observation is contradicted by experimental studies, which are only able to identify one reflection configuration for any set of flow conditions. Consequently, three-shock theory is incapable of predicting the actual height of the Mach stem. Ben-Dor et al. [1] have stated that identifying the precise factors determining the size of a Mach reflection remains one of the last unresolved shock wave reflection problems in the steady flow field.

Hornung et al. [2] introduced the concept of the normalized Mach stem height. In their model, it is assumed that the downstream pressure is sufficiently low, and the normalized exit cross-sectional area at the trailing edge sufficiently large, that supersonic flow is established at the downstream end of the stream tube between the two slipstreams. In their study, it was concluded that the normalized Mach stem height is dependent on the specific heat ratio, γ, the inflow Mach number, M_0, the wedge angle, θ_w, and the normal exit cross-sectional area at the trailing edge, h_t. However, the precise relationship between these parameters was not clarified.

Azevedo et al. [3] presented a physical model to predict the Mach stem height. In this model, it was assumed that: (1) the Mach stem is straight and perpendicular to the symmetry plane, (2) the Mach stem, the slipstream, and the symmetry plane form a one-dimensional converging nozzle, (3) the sonic throat in the converging nozzle is located at the leading characteristic of the expansion fan intersection with the slipstream, (4) the flow behind the Mach stem inside the converging nozzle is isentropic and attains sonic conditions at the throat, and finally (5) the gas is an ideal fluid. By applying the conservation of mass and linear momentum, an analytical model was developed, which enabled calculation of the Mach stem height. However, some researchers have questioned the validity of the model. For example, the actual Mach stem tends to be curved rather than straightened. Furthermore, in the study performed by Vuillon et al. [4] to determine the location of the sonic throat, it was clearly demonstrated that the sonic throat is not located at the intersection of the leading characteristic of the expansion fan and the slipstream.

In a later study, Li et al. [5] modified the model of Azevedo et al. [3] for predicting the Mach stem height of Mach reflection wave configurations in steady flows. Their

Communicated by K. Takayama

T. I Tseng · R. J. Yang (✉)
Department of Engineering Science, National Cheng Kung University, Tainan 70101, Taiwan
E-mail: rjyang@mail.ncku.edu.tw

study consider the interactions of the expansion fan with the reflected wave and the slipstream, and made the assumptions that the Mach stem was slightly curved and that the sonic throat in the converging nozzle was located at actual location. In both the Li and Ben-Dor's model and Azevedo and Liu's model, when the Mach stem height is forced to be zero the shock wave angle must conform to the van Neumann criterion. However, the transition angle yielded by the model proposed by Azevedo and Liu is actually greater than the von Neumann transition angle since it incorrectly specifies the throat location.

The Models of Azevedo and Liu and Li and Ben-Dor both assumed that the flow was free of downstream influence. However, Schotz et al. [6] proposed a more realistic model for predicting the height of the Mach stem in steady flows by accounting for the trailing edge angle of the reflecting wedge and by taking into consideration the expansion fan and its interaction with both the reflection wave and the slipstream. Using this model, it was determined that the normalized Mach stem height increases as the trailing edge angle increases. In other words, their results suggested that the downstream flow expansion process might have a significant influence upon the Mach stem height. Ben-Dor et al. [7] adopted both numerical and experimental approaches to investigate the same problem, and indicated that there was no significant change in the Mach reflection configuration for any of the considered trailing edge angles. Similarly, the experimental results of Chpoun et al. [8] also contradicted the analytical findings of Schotz et al. [6].

From the discussion above, it is clear that the precise influence of the downstream geometry and flow conditions on the Mach stem height in supersonic flow is yet to be fully clarified. Hence, the present study employs the unique Space-Time Conservation Element and Solution Element (CE/SE) method developed by Chang et al. [9] to further investigate this problem. The following section of this paper provides a brief description of the adopted numerical method. The paper then presents a validation of the computer code, and subsequently provides some results and discussion. Finally, the paper presents some brief conclusions.

2 Numerical method

Chang et al. [9] proposed the original CE/SE method, which uses triangular and tetrahedral meshes to solve conservation laws. Subsequently, Zhang et al. [10] introduced a modified two-dimensional CE/SE method employing quadrilateral and hexahedral meshes. The CE/SE method incorporates many unconventional features, including a unified treatment of space and time in calculating flux conservation, a new shock-capturing strategy which does not use a Riemann solver, and simple treatments of the reflective and nonreflective boundary conditions based on a local space-time flux conservation. In the CE/SE method, the flow variables, U, and its spatial gradient, U_x and U_y, are considered to be unknowns and are solved simultaneously. Recently, the CE/SE method has been employed in numerical investigations of a wide variety of flow problems, including various acoustic problems (Wang et al. [11]), shock/acoustic wave interaction (Wang et al. [12]), and chemically reacting flows (Yu et al. [13]). In the case of shock/acoustics interaction, although the shock pressure jump is several orders of magnitude higher than the acoustic wave pressures, the CE/SE method is still capable of catching the penetrated acoustic waves behind the shocks. The CE/SE method is without doubt a promising numerical framework for the investigation of fluid mechanics problems at all flow velocities.

3 Results and discussion

3.1 Code validation

Consider a diverging nozzle whose cross-sectional area is specified as

$$A(x) = 1.398 + 0.0347x[\tanh(4.) - \tanh(-4.)] \quad (1)$$

The nozzle entrance is located at $x = 0$ and the exit at $x = 10$. The fluid within the nozzle is assumed to be air with a specific heat ratio of 1.4. It is chosen to validate the code under the supersonic inflow and subsonic outflow boundary conditions, the inflow properties can be specified as:

$$M_0 = 1.5, \quad \rho = 1.4, \quad \text{and} \quad p = 1.0 \quad (2)$$

The flow at the outlet is subsonic, and hence the pressure at the exit is a constant given by $p = 2.459$.

All of the flow property values within the domain are specified to equal those of the inflow values. Figure 1 compares the analytical and numerical solutions of pressure, density, and Mach number distributions along the central line. It is apparent that the pressure specified at the exit creates a normal shock in the converging nozzle. In front of the normal shock, the density and pressure are seen to decrease, and the Mach number to increase, as the cross-sectional area increases. However, behind the normal shock, the flow is subsonic and the pressure increases to match the exit pressure. With subsonic flow at the exit, the exit pressure is equal to the specified outlet pressure. It is noted that

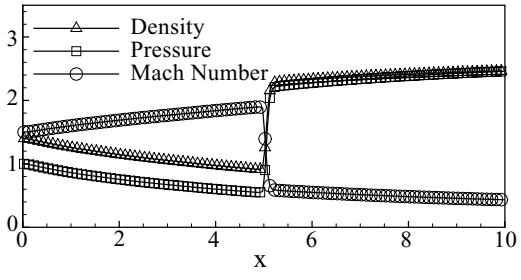

Fig. 1 Comparison of analytical and numerical results for flow in a convergent nozzle

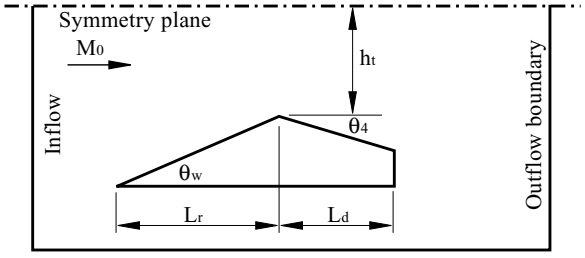

Fig. 2 Computational domain and boundary conditions

the shock discontinuity is well resolved almost within few mesh intervals. In the present numerical simulation using the CE/SE method, it can be seen that there is excellent agreement between the numerical results and the analytical solutions when appropriate boundary conditions are specified.

3.2 Mach steam height with different downstream duct length

Figure 2 presents a schematic illustration of a supersonic flow entering a duct with an embedded wedge. Under these conditions, different downstream duct lengths of the reflecting wedge (L_d) may change the location of the second expansion. The following investigation explores the influence of different length ratios, R (where $R = L_d/L_r$), on the flow configuration.

Initially, the Mach reflection configuration was modeled for an inflow Mach number of 2.84, a distance between the trailing edge and the symmetry plane of 0.5, a length ratio of 0.4, and a reflecting wedge angle of 22°. In this particular simulation case, the trailing edge angle, θ_4, was specified to be 0. It is noted that the space underneath the wedge was also included in the computation. Since the problem is symmetrical in nature, it was only necessary to perform computations in one-half of the modeled geometry. Two sets of unstructured grids were generated to conduct a refinement study for the coarse mesh (34,000 cells)and finer mesh (102,000 cells), respectively. From the result adopting a finer mesh slightly improves the numerical results, however, the coarse mesh also provides a satisfactory representation of the Mach reflection structure. Furthermore, it is observed that the Mach reflection structure and the reflecting point by the reflected wave at the same locations in the vicinity of the symmetry plane and reflecting wedge, respectively. Consequently, the computational results presented in the following paragraphs are obtained using the finer gird configuration.

The following configuration was modeled for a reflecting wedge angle of 22°, an inflow Mach number of $M_0 = 2.84$, the length ratio of $R = 0.4$, and two different values of h_t, i.e. $h_t = 0.5$ and 0.6. The corresponding numerical results are shown in Fig. 3a and b, respectively. In both cases, the results indicate that the modeled shock reflection is the Mach reflection configuration. The oblique shock waves generated by the leading edge of the reflecting wedge, and the Mach reflection configuration formed

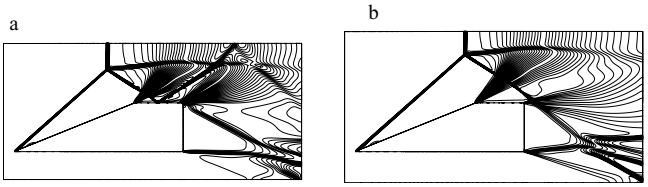

Fig. 3 Flow evolutions with $M_0 = 2.84$, $\theta_w = 22°$, $R = 0.4$ for different values of h_t: **(a)** $h_t = 0.5$; and **(b)** $h_t = 0.6$

at the neighboring symmetry plane, are clearly shown in the figure. The expansion fans emanating from the trailing edge first refract through the reflected shock and then interact with slipstream. The flow becomes subsonic after the Mach stem and is then accelerated in the convergence nozzle formed by the slipstream and the symmetry plane. In the Fig. 3a and b, the reflected shock refracts with expansion and subsequently impacts the reflecting wedge, hence causing a second shock reflection, i.e., regular reflection. When this shock wave subsequently interacts with the slipstream, the re-reflected wave is transmitted through the slipstream and forms a shock reflection at the symmetry plane. Since the geometry of the wedge is such that its upper right external angle exceeds the maximum permissible value of Prandtl–Meyer expansion, a separation zone is formed behind the reflecting wedge. The flow within this separation zone is subsonic. Furthermore, curved shear layers are evident around the separation zone. The external flow is supersonic, and the curved shear layer causes a continuous flow compression to take place in the vicinity of this layer. The compression waves gradually converge and coalesce to form a finite oblique shock wave. It is noted that the Mach reflection moves in the downstream direction for the higher value of h_t. Hence, the reflected shock wave does not impact the reflecting wedge, but interacts with the shear layer instead. Since the separation zone is subsonic, the reflected shock wave is unable to pass through the shear layer into the separation zone. Furthermore, the external flow near the shear layer is smoothly turned by the interaction of the expansion fan and the reflected wave. Consequently, the reflected shock vanishes when it interacts with the shear layer.

Figure 4 presents the variation in the normalized Mach stem height with the length ratios (R) for different distances between the trailing edge and the symmetry plane (h_t). It is observed that for a given value of h_t the normalized Mach

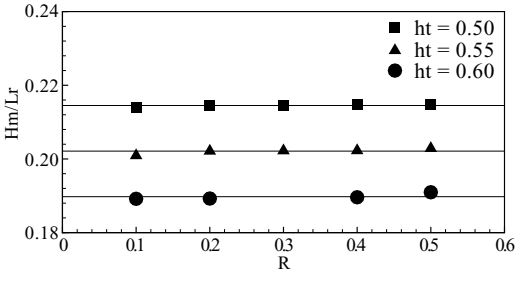

Fig. 4 Variation of normalized Mach stem height with length ratio for different h_t

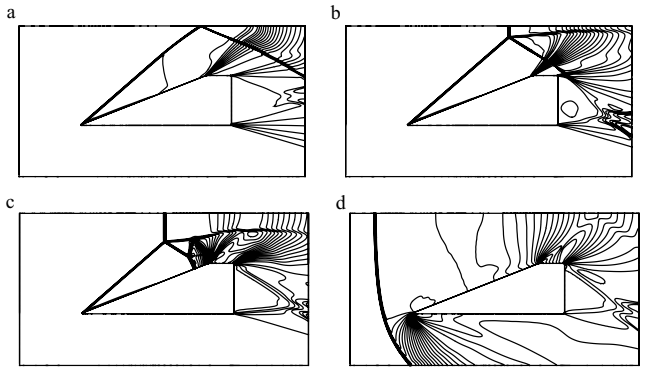

Fig. 5 Transition process of bow shock wave: **(a)** nonstationary regular reflection configuration; **(b)** nonstationary Mach reflection configuration; **(c)** secondary Mach reflection configuration; and **(d)** stationary bow shock wave in front of the reflecting wedge

stem height remains virtually constant for different length ratios, i.e., its height is independent of the length ratio. Furthermore, the Mach stem height is seen to increase as the value of h_t becomes smaller. The Mach reflection structure remains stable as the distance between the trailing edge and symmetry plane decreases until the reflected shock impacts the reflecting wedge. At this point, the subsonic region behind the Mach stem become unstable and the triple point moves in the upstream direction along the incident shock wave. Finally, the Mach stem moves upstream and become a bow shock wave in front of the reflecting wedge. A typical example of this transition process is shown in Fig. 5a–d, which represent the case of an inflow Mach number of $M_0 = 2.84$, an incident shock wave angle of $\Phi_1 = 41°$ (reflecting wedge angle $\theta_w = 21.529°$), and a normalized distance between the trailing edge and the symmetry plane of $h_t/L_r = 0.4$. Figure 5a–d illustrates the nonstationary regular reflection configuration and the Mach reflection configuration, respectively. In Fig. 5a–c, it can be seen that the reflected shock wave impacts the reflecting wedge and that Mach stem moves upstream, hence causing a secondary Mach reflection. Finally, Fig. 5a–d shows that a stable bow shock wave is established in front of the reflecting wedge. It is noted that these results are in good agreement with the previous studies of Vuillon et al. [14].

3.3 Mach stem height with different trailing edge angles

Hornung et al. [2] suggested that the normalized Mach stem height is dependent on the incident shock wave angle (Φ_1). Furthermore, Vuillon et al. [14] stated that the extent of the expansion fan was influenced by the trailing edge angle, θ_4, and hence brought about changes in the Mach stem height. It was noted that for a constant trailing edge angle, larger incident shock wave angles would result in a larger Mach stem height.

The corresponding computational domain has been presented previously in Fig. 2. In the present investigation of the influence of the trailing edge angle upon the Mach stem

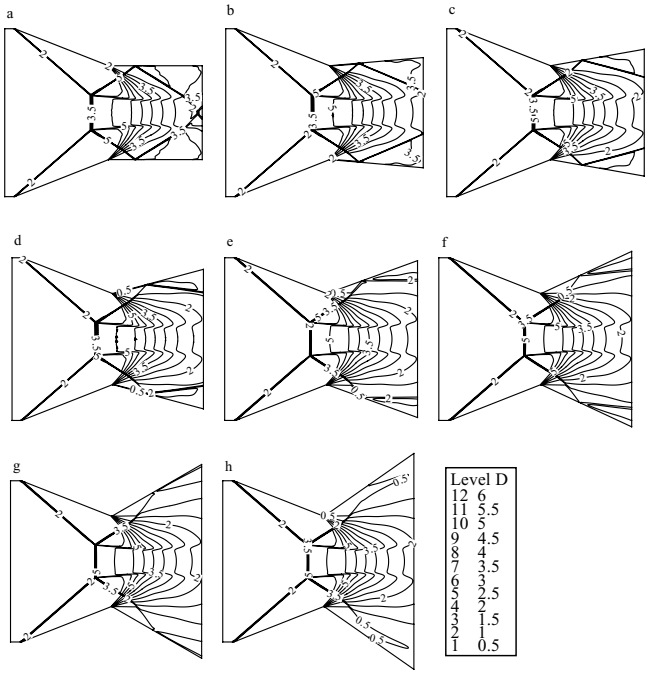

Fig. 6 Numerical density contours for $M_0 = 2.84$ and trailing edge angles of: **(a)** $\theta_4 = 0°$; **(b)** $\theta_4 = 5°$; **(c)** $\theta_4 = 10°$; **(d)** $\theta_4 = 15°$; **(e)** $\theta_4 = 20°$; **(f)** $\theta_4 = 25°$; **(g)** $\theta_4 = 30°$; and **(h)** $\theta_4 = 35°$

height, the following boundary conditions were imposed: (1) supersonic conditions on the upstream inflow, (2) reflective conditions on the symmetry plane and wedge surface, and (3) nonreflective conditions on the downstream outflow. Figure 6a–h presents the simulation results obtained for different values of trailing edge angles for the case of an inflow Mach number of $M_0 = 2.84$, a reflecting wedge angle of $\theta_w = 21.529°$, a normalized distance between the trailing edge and the symmetry plane of $h_t/L_r = 0.5$, and the trailing edge angles of $\theta_4 = 0°$, 5°, 10°, 15°, 20°, 25°, 30°, and 35°, respectively. The individual figures illustrate various details of the flow structures, including the incident shock wave, the reflected shock wave, the Mach stem, the slipstream, the trailing edge expansion, and the downstream flow acceleration through the converging nozzle. The results clearly demonstrate that the Mach stem height is independent of the trailing edge angle.

In order to investigate the influence of the distance between the trailing edge and the symmetry plane on the Mach stem height, two different distances are considered, i.e., 0.45 and 0.5. Figure 7a–c respectively illustrate the variation of the normalized Mach stem height (i.e. H_m/L_r), the location of the sonic throat (i.e. X_t/L_r), and the location of the Mach stem (i.e. X_m/L_r) with the trailing edge angle for different values of incident shock wave angle and distances between the trailing edge and the symmetry plane. Figure 7a–c indicates that the Mach stem height is independent of the trailing edge angle, and hence it can be concluded that the trailing expansion process does not affect the Mach stem height. These results are in good agreement with the previous numerical studies of Ben-Dor et al. [1] and experimental

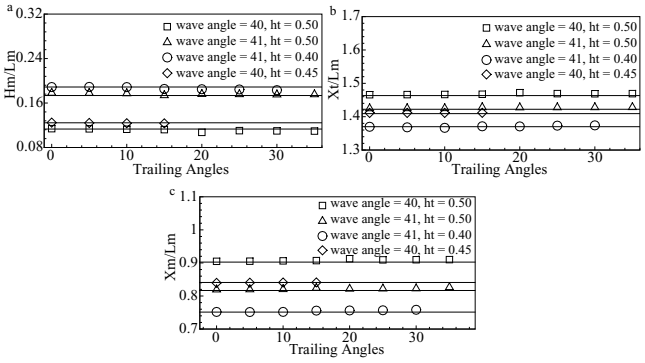

Fig. 7 Variation of **(a)** normalized Mach stem height, **(b)** normalized sonic throat location, and **(c)** normalized Mach stem location with trailing edge angle for different incident shock wave angles and different distances between the trailing edge and the symmetry plane

works of Chpoun et al. [8]. Furthermore, decreasing the incident shock wave angle or increasing the distance between the trailing edge and the symmetry plane is seen to cause the sonic throat and the Mach stem to move downstream. From these results, it can be concluded that the Mach stem height increases as either the incident shock wave angle increases or the distance between the trailing edge and the symmetry plane decreases. As the distance between the trailing edge and the symmetry plane decreases, the normalized Mach stem moves in the upstream direction and increases in height.

4 Conclusion

This study has employed the Space-Time Conservation Element and Solution Element (CE/SE) method to investigate the characteristics of Mach reflection (MR) in two-dimensional supersonic flows. Prior to presenting the computed MR results, the CE/SE method has also been validated through comparisons with analytical solutions for the flow configuration in the diverging nozzle for supersonic inflow and subsonic outflow conditions.

In Sect. 3.2, the space underneath a reflecting wedge is included in the calculation. The parameter, length ratio (R), is used to investigate its effect on the Mach stem height. Both the expansion fans at the top of the wedge and the end of the duct interact with the slipstream and reflection shocks. The subsonic patch behind the Mach stem is isolated in the region between the Mach stem and the slipstream. The subsonic patch is not influenced by the second expansion fan near the end of the duct. This length ratio, therefore, has no influence on the Mach stem height. In Sect. 3.3, the effect of trailing edge angles on the Mach stem height is studied. It has been shown that the trailing edge angles do not affect the Mach reflection configuration either. Hence, it can be concluded that the Mach reflection configuration is free of downstream influences if the downstream flows are generally supersonic except for the small subsonic patch, then manipulating the tail of the expansion fan within the supersonic region by changing the boundary cannot have an influence on the upstream flows. The present results provide an independent clarification of the inconsistent solutions provided by Ben-Dor et al. [1] and by Schotz et al. [6]. It has been determined that the present solutions are in good agreement with those of Ben-Dor et al. The CE/SE method has successfully demonstrated its capability in simulating MR phenomena.

Acknowledgements The authors gratefully acknowledge the support provided to this study by the R.O.C. National Science Council, under the grant of NSC 91-2212-E006-127. Particular appreciation is also extended to S. C. Chang, S. T. John Yu, Z. C. Zhang, and X. Y. Wang for their invaluable input regarding CE/SE methods.

References

1. Ben-Dor, G., Takayama, K.: The phenomena of shock wave reflection—a review of unsolved problems and future research needs. Shock Waves **2**, 221–223 (1992)
2. Hornung, H.G., Robinson, M.L.: Transition from regular to Mach reflection of shock waves. Part 2. The steady-flow criterion. J. Fluid Mech. **123**, 155–164 (1982)
3. Azevedo, D.J., Liu, C.S.: Engineering approach to the prediction of shock patterns in bounded high-speed flows. AIAA J. **31**, 83–90 (1993)
4. Vuillon, J., Zeitoun, D., Ben-Dor, G.: Numerical investigation of shock wave reflections in steady flows. AIAA J. **34**, 1167–1173 (1996)
5. Li, H., Ben-Dor, G.: A parametric study of Mach reflection in steady flows. J. Fluid Mech. **341**, 101–125 (1997)
6. Schotz, M., Levy, A., Ben-Dor, G., Igra, O.: Analytical prediction of the wave configuration size in steady flow Mach reflections. Shock Waves **7**, 363–372 (1997)
7. Ben-Dor, G., Elperin, T., Li, H., Vasiliev, E., Chpoun, A., Zeitoun, D.: Dependence of steady Mach reflections on the reflecting-wedge trailing-edge angle. AIAA J. **351**, 1780–1782 (1997)
8. Chpoun, A., Leclerc, E.: Experimental investigation of the influence of downstream flow conditions on Mach stem height. Shock Waves **9**, 269–271 (1999)
9. Chang, S.C., Wang, X.Y., Chow, C.Y.: The space-time conservation element and solution element method: a new high resolution and genuinely multidimensional paradigm for solving conservation laws. J. Comput. Phys. **156**, 89–136 (1999)
10. Zhang, Z.C., Yu, S.T., John Chang, S.C.: A space-time conservation element and solution element method for solving the two-dimensional and three-dimensional unsteady Euler equations using quadrilateral and hexahedral meshes. J. Comput. Phys. **175**, 168–199 (2002)
11. Wang, X.Y., Chow, C.Y., Chang, S.C.: Numerical simulation of gust generated aeroacoustics in a cascade using the space-time conservation element and solution element method. AIAA Paper 98–0178 (1998)
12. Wang, X.Y., Chang, S.C., Jorgenson, P.C.E.: Accuracy study of the space-time CE/SE method for computational aeroacoustics problems involving shock waves. AIAA Paper 2000–0474 (2000)
13. Yu, S.T., Chang, S.C.: Applications of the space-time conservation element/solution element method to unsteady chemically reactive flows. AIAA Paper 97–2099 (1997)
14. Vuillon, J., Zeitoun, D., Ben-Dor, G.: Reconsideration of oblique shock wave reflections in steady flows. Part 2. Numerical investigation. J. Fluid Mech. **301**, 37–50 (1995)